

# Transient, Three-Dimensional Potential Flow Problems and Dynamic Response of the Surrounding Structures. Part I: Description of the Fluid Dynamics by a Singularity Method (Computer Code SING)

R. KRIEG AND G. HAILFINGER

*Kernforschungszentrum Karlsruhe GmbH, Institut für Reaktorentwicklung,  
Postfach 3640, 7500 Karlsruhe, Federal Republic of Germany*

Received May 12, 1978

In Part I a singularity method—also called boundary integral equation method or panel method—has been developed. It is applicable especially to highly transient internal flow problems with any three-dimensional geometry including walls wetted on both sides. The boundary conditions are prescribed in terms of pressures and/or accelerations. The method is primarily based on a recently developed dipole element treatment for incompressible fluids. Such elements (panels) can be fitted to the fluid boundary or any enveloping surface. Also, point sources may be included. The applicability of the method is demonstrated by two different examples: the incipient flow in a T-joint and the oscillating flow in the pressure suppression system of a boiling water reactor. In Part II the coupling of the transient flow problem with the dynamic behavior of the surrounding structure will be investigated.

## 1. INTRODUCTION

Future advanced safety criteria of large technical systems will, in many cases, require a catastrophic failure to be ruled out even in cases with postulated failures of single components. As a consequence, the impact of a failing structural member on the other parts of the system must be thoroughly investigated. In many cases these structural members are surrounded by fluid which takes part in the dynamic processes. Thus, there is an increasing demand for analysis methods for complex mechanical systems including fluid fields and structural members, both under highly transient conditions.

Various applications for such advanced investigations arise from problems in nuclear reactor safety. Examples are the seismic loading of fluid containers, rapid shut off in coolant circuits, the postulated breach of a coolant circuit with subsequent loading of pressure vessel internals, and the steam condensation in the pressure suppression system of a boiling water reactor.

In this part of the paper a singularity method<sup>1</sup> is presented which is applicable to the fluid dynamics aspects of the above problems. In Part II the fluid dynamic model

<sup>1</sup> Methods of this type are also known under the term "boundary integral equation method (BIE)" or "panel method."

is integrated into the mathematical description of the structural response in order to account for the mutual dependency—called coupling—between fluid and structural dynamics. In this way the conditions for both the fluid and the structural dynamics are simultaneously satisfied.

In order to demonstrate the applicability of the singularity method the incipient flow in a T-joint with rectangular cross sections is investigated. Another, more detailed example is the water pool of the above-mentioned pressure suppression system.

## 2. DEFINITION OF THE PROBLEM

The fluid dynamic parts of those problems which have been referred to in Section 1 may be characterized as follows:

- highly transient flow fields
- almost arbitrary three-dimensional flow fields, especially internal flow problems with thin walls wetted on both sides
- boundary conditions with prescribed normal velocities (Neumann type) or with prescribed pressures (free fluid surface, Dirichlet type).

Furthermore, the mathematical description for the fluid dynamics must be useful as a basis for a solution procedure in coupled problems in Part II of this paper.

In order to solve the fluid dynamics problems defined above, some restrictions are necessary or advisable:

- Displacements of the fluid boundaries must be small in comparison to characteristic dimensions of the fluid field.
- The dynamic pressures due to the fluid velocity at a fluid boundary with prescribed pressures must be small in comparison to characteristic pressure differences of the system.
- Body forces, for instance gravity forces, cannot be taken into account. (However, by applying the technique of fluid structural coupling surface waves can be modeled.)
- The fluid viscosity must be negligible.
- The fluid compressibility must be negligible and the fluid density must be constant. (However, by applying the technique of fluid structural coupling the fluid compressibility may be roughly approximated by additional artificial boundary flexibilities.)
- Fluid rotations must be negligible.

In contrast to steady-state flow problems the neglect of the fluid viscosity in transient flow problems seldom introduces large errors for two reasons. First, at each fluid point the viscosity force must be compared not only with the convective inertia (as in the case of steady-state flows), but also with the local inertia which is proportional to the transient flow changes. Second, most transient problems concern

incipient flows with lower velocities than in corresponding steady-state problems. Furthermore, viscosity effects are usually proportional to the square of the velocities. Consequently, if potential flow theory (flow without viscosity) is adequate for many steady-state problems, as indicated in the next section, it will be even more adequate for highly transient problems.

More questionable is the neglect of the fluid compressibility. For steady-state flows this means that the Mach number must be sufficiently small (according to [3] smaller than 0.5). For transient flows it means, in addition, that the propagation velocity of compression waves (velocity of sound) is assumed to be infinite (Surface waves or wave effects due to flexible boundaries, which are important in the case of coupled problems, are not directly affected.) In other words, the time necessary for a compression wave to traverse the fluid region is neglected. If this time is small in comparison to the times for the transient flow changes, then the above assumption is justified [1].

### 3. BASIC CONCEPT OF THE SINGULARITY METHOD

Under the assumptions of Section 2 the three-dimensional flow and pressure fields of the problem may be generated by superposition of elementary flow and pressure fields which can be described by simple analytical functions. Examples for such elementary fields are source flows, dipole flows, or—more general—flows due to singularities. Now, assuming that these singularities may be distributed over the fluid field boundary or any other given boundary enclosing the fluid region, the intensity distribution for the singularities can be found by satisfying the boundary conditions. This requires the solution of an integral equation. The unknowns occurring here refer only to the fluid boundary. For numerical solution the singularity distribution is approximated by an appropriate arrangement of panels—sometimes also called finite elements—with prescribed distribution shapes. As a consequence, the singularity distribution is described by a finite number of unknowns and the integral equation is reduced to one linear equation for each boundary point. In general a unique solution can be obtained, when the number of unknowns is the same as the number of linear equations. Thus, an exact satisfaction of the boundary conditions can be achieved only at a finite number of boundary points. This is the basic concept of the singularity method which will be used in this paper. A more general description may be found in contributions from Wait and Symm in [2].

The same basic concept is widely used in aerodynamics. Here, some of the first papers including extensive applications have been published by Hess and Smith [3–5]. A description of these works may also be found by Lock in [6]. Other applications in aerodynamics are reported, for instance, by Johnson and Rubbert [7], by Medan [8], by Grodtkjaer [9], and by Körner and Hirschel [10]. Investigations of ship hulls and applications to submarine problems are reported by Ecer, Eichers, and Bratanow [11], by Albring and Schindler [12], and by Webster [13].

All of these papers deal with external steady-state flow problems, namely, flows

around wings, fuselages, or ship hulls. Usually the applied singularities are sources uniformly distributed over plane triangular, or quadrilateral panels which approximately form the fluid boundary. One way to improve the accuracy of the method is the application of panels with curved surfaces (avoiding sharp corners between adjacent panels) in combination with linearly varying source distributions [5, 7], or the application of higher-order approximations as discussed by Argyris and Scharpf [14] or by Nedlec [15]. Another way to improve the accuracy is to distribute the singularities at a certain distance outside the fluid field [13, 16, 17].

The situation is different for the so-called interior flow problems, i.e., flows in channels or containers, which are dealt with in this paper. Useful results have been obtained with point singularities in a certain distance from the fluid boundary by Höller [18], Landweber [19], and one of the authors [20]. But this method cannot be used for fluid fields with thin walls wetted on both sides, as required here, and there are, besides, some questions and difficulties concerning optimal locations of the singularities. On the other hand, applying a panel method with distributed sources at the fluid boundaries is impossible or unsuitable for three reasons. Again, thin walls wetted on both sides cannot be treated adequately, since fluid sources are not able to model a pressure step across the wall. Furthermore, considerable leakages at boundary edges are reported by Renken [21]. Finally, depending on the geometric details, internal flow problems have a larger tendency than external flow problems to yield ill-conditioned systems of linear equations.

Therefore a modified singularity method has been developed, the numerical calculations are performed using a computer code called SING1. As singularities so-called dipole elements are used. These are rectangular plane panels with uniformly distributed dipoles (or doublets). The dipole axes are perpendicular to the panels. The pressure field induced by such a dipole element is continuous over the whole space, except in the panel itself, across which a pressure step occurs. For this reason dipole elements are especially suitable for modeling the pressure differences at thin walls which are wetted by the fluid on both sides. Detailed investigations reveal another advantage: excessive leakages at boundary edges, which arise when source elements form the fluid boundary, do not occur. Finally, for dipoles the decay of pressure and velocity with increasing distance is one order higher than in the case of fluid sources. This fact seems to reduce the tendency to produce ill-conditioned systems of linear equations observed for internal flow problems treated by source elements.

A disadvantage of dipole elements is that the analytical functions describing the pressure and velocity distributions are somewhat more difficult to handle than the corresponding distributions from the well-known source elements. For this reason, only rectangular, but not triangular, dipole elements are available in SING1. Consequently, the discretization of curved fluid boundaries may create some difficulties.

To overcome these difficulties, but also to allow for a flexible and economical treatment of the given problems, two additional options can be used in SING1.

For fluid boundaries not generated by thin walls wetted on both sides the dipole elements may be applied in a submerged version. This increases the smoothness and the accuracy of the results, provided the distance between dipole element and fluid boundary is not too large. Moreover, the intensity of each dipole element need not be introduced as an unknown of the system of linear equations. Instead several intensities may be described by the same unknown or by the weighted mean of any four unknowns. This allows for an approximation of curved fluid boundaries by a large number of rectangular panels. The number of unknowns, however, may be kept relatively small.

In comparison to finite-difference methods, see for instance [22–24], the application of singularity methods offers some advantages:

—Only the fluid boundary and not the whole three-dimensional fluid domain has to be discretized for numerical treatment.

—Concentrating the discretization at the fluid boundary allows for an optimal formulation of the boundary conditions. To gain similar advantages in the case of applying finite-difference methods, curvilinear coordinate systems must be introduced having coordinate surfaces coincident with the fluid boundaries [25, 26].

—Under the assumptions of inviscid and incompressible conditions an “exact” solution is obtained for boundary conditions which differ slightly from the given conditions. But these deviations are calculated as a part of the solution. Their average values over certain subregions of the fluid boundary vanish.

—Since in this singularity method the fluid dynamic unknowns are related only to the fluid boundary, and this boundary largely coincides with the surfaces of the surrounding structures, the development of solution techniques for coupled fluid-structural dynamics problems is facilitated.

—A structural disadvantage inherent in the singularity method is that effects due to fluid viscosity are neglected. Effects due to fluid compressibility may be roughly included if required. Furthermore, the fluid density must be uniform throughout the whole fluid region.

—However, the fact that in singularity methods it is primarily the flow conditions at the fluid boundary which are computed, turns out to be rather an advantage than a disadvantage, since in most cases it is just these conditions which are of interest.

#### 4. FLUID DYNAMIC EQUATIONS

The field equations which govern an inviscid, incompressible fluid without sources and body forces are

$$\operatorname{div} \bar{v} = 0 \quad (\text{continuity}) \tag{4.1}$$

and

$$\frac{d}{d\tau}(\bar{v}) = -\frac{1}{\rho} \operatorname{grad} p \quad (\text{momentum}),$$

where  $\bar{v}$  is the velocity vector;  $\tau$ , time;  $\rho$ , density;  $p$ , (static) pressure. Introducing the total pressure  $P$  as a new variable

$$P = p + \frac{1}{2}\rho\bar{v}^2, \quad (4.2)$$

using the identity

$$\frac{d}{d\tau}(\bar{v}) = \frac{\partial}{\partial\tau}(\bar{v}) + (\bar{v}\nabla)\bar{v} = \frac{\partial}{\partial\tau}(\bar{v}) + \frac{1}{2}\text{grad}\bar{v}^2 - \bar{v} \times \text{rot}\bar{v},$$

and assuming

$$\text{rot}\bar{v} = 0,$$

the basic equation can be stated as

$$\text{div}\bar{v} = 0 \quad (4.3)$$

$$\frac{\partial\bar{v}}{\partial\tau} + \frac{1}{\rho}\text{grad}P = 0.$$

In these equations the unknowns  $\bar{v}$  and  $P$  appear linearly. Therefore the principle of superposition, which is the basic idea of the method of singularities, is applicable.

It should be mentioned that this is not true for the unknowns  $\bar{v}$  and  $p$  in Eqs. (4.1), since the time derivatives are related to local coordinate systems which are translating and rotating according to the velocity field  $\bar{v}$ . For different flow fields this means that the local coordinate systems translate and rotate in different ways. However, for superposition of different flow fields a major prerequisite is that the quantities to be superimposed must be related to the same coordinate system.

In order to make use of the linearity of Eqs. (4.3) and to use the principle of superposition to solve the problem, the boundary conditions should also be linear functions of  $\bar{v}$  and  $P$ . This is true for flow problems with boundaries represented by rigid walls (for instance the aerodynamic problems mentioned in Section 3), but not for flow problems with free fluid surfaces,<sup>2</sup> where the pressure  $p$  and not the pressure head  $P$  is given.

Fortunately, in many cases the velocities at free fluid surfaces are rather small, so that

$$\frac{1}{2}\rho\bar{v}_f^2 \ll p_0,$$

where  $\bar{v}_f$  is the velocity vector at the free fluid surface and  $p_0$  is the characteristic pressure difference occurring in the problem. Under this condition the term  $\frac{1}{2}\rho\bar{v}^2$  is negligible at these boundaries and the prescribed pressures  $p$  may be simply approximated by prescribed total pressures  $P$ .

<sup>2</sup> Here a free fluid surface is any fluid boundary with prescribed pressure.

In other cases with somewhat larger velocities at the free fluid surface, one or more computational steps may be added, where the approximation of the prescribed pressures  $p$  may be iteratively improved on the basis of the velocities at the free fluid surface obtained in the preceding computational step.

5. PRESSURE AND ACCELERATION FIELDS DUE TO A RECTANGULAR DIPOLE ELEMENT

The formulas describing the pressure and velocity distributions around a rectangular dipole are given in [27]. Here only some major steps in deriving these formulas are repeated.

In highly transient flow problems the fluid accelerations, rather than the velocities, are of primary interest. Therefore the acceleration vector  $\bar{a}$

$$\bar{a} = \partial \bar{v} / \partial \tau \tag{5.1}$$

is introduced. It should be emphasized that for this definition which is based on the partial, and not as usually on the total, time derivatives, inertia forces are not proportional to the acceleration vector  $\bar{a}$ .

In order to present the solutions of the fluid dynamic equations (4.3) for a discrete source or a dipole surrounded by an infinite fluid, a spherical coordinate system  $r, \psi, \phi$  is introduced. The directions of the components  $a^r, a^\psi, a^\phi$  of the acceleration vector  $\bar{a}$  are shown in Fig. 1. For a source  $S$  located at the origin of the spherical coordinate system the pressure and acceleration fields are

$$\begin{aligned} P &= \rho \frac{\partial S / \partial \tau}{4\pi} \frac{1}{r}, & a^\psi &= 0 \\ a^r &= \frac{\partial S / \partial \tau}{4\pi} \frac{1}{r^2}, & a^\phi &= 0. \end{aligned} \tag{5.2}$$

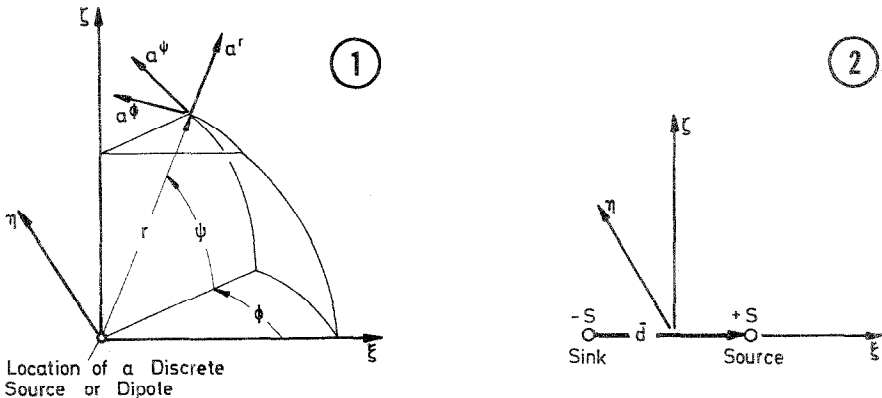


FIG. 1. Spherical coordinate system with a discrete source or dipole.

FIG. 2. Definition of the dipole  $\bar{T}$ .

The dipole  $\bar{T}$  is defined as

$$\bar{T} = \lim_{d \rightarrow 0} S\bar{d}.$$

As shown in Fig. 2, a source and a sink, both of intensity  $S$ , are separated by distance  $\bar{d}$ . According to these definitions the pressure and acceleration fields of a dipole  $T$  can be calculated by superimposing the corresponding fields due to both singularities with the distance vector  $\bar{d}$  approaching zero. The results are

$$\begin{aligned} P &= \rho \frac{\partial T / \partial \tau}{4\pi} \frac{1}{r^2} \cos \psi \cdot \cos \phi, & a^\psi &= \frac{\partial T / \partial \tau}{4\pi} \frac{1}{r^3} \sin \psi \cdot \cos \phi, \\ a^r &= 2 \frac{\partial T / \partial \tau}{4\pi} \frac{1}{r^3} \cos \psi \cdot \cos \phi, & a^\phi &= \frac{\partial T / \partial \tau}{4\pi} \frac{1}{r^3} \sin \phi. \end{aligned} \tag{5.3}$$

Equations (5.2) and (5.3) are valid through the whole space except the coordinate origin, where the singularities, i.e., the source or the dipole, are located. By integration over the surface of a small sphere surrounding the dipole, a force can be found which is proportional to  $\partial T / \partial \tau$  and has the same direction as  $\bar{T}$ .

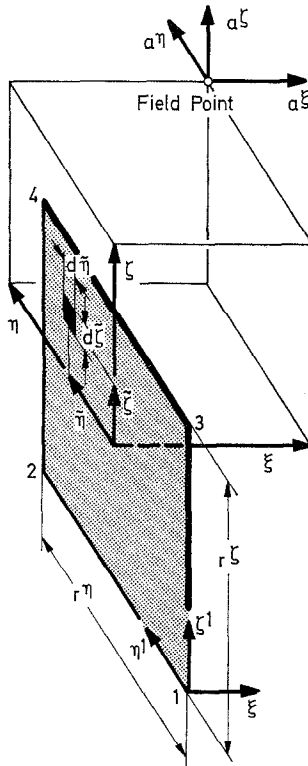


FIG. 3. Cartesian coordinate system with rectangular dipole element.



Now dipoles will be uniformly distributed over a plane rectangular element shown in Fig. 3. The dipole axes are perpendicular to the element. Field points are described by Cartesian coordinates  $\xi, \eta, \zeta$ ; points belonging to the plane rectangular dipole element are described by the coordinates  $\tilde{\eta}, \tilde{\zeta}$ . The origin of both coordinate systems is located at the element center and the  $\eta$  and  $\zeta$  axes and  $\tilde{\eta}$  and  $\tilde{\zeta}$  axes, respectively, are perpendicular to the element length  $r^n$  and element width  $r^t$ . The symbols  $a^\xi, a^n, a^t$  denote the corresponding components of the acceleration vector  $\vec{a}$ . Introducing the dipole density

$$t = \frac{d^2 T}{d\tilde{\eta} d\tilde{\zeta}} \quad (5.4)$$

and using appropriate formulas for coordinate transformation between the system  $r, \psi, \phi$  and the system  $\xi, \eta, \zeta$ , the principle of superposition yields

$$\begin{aligned} P &= \rho \frac{\partial t / \partial \tau}{4\pi} \int_{-r^t/2}^{+r^t/2} \int_{-r^n/2}^{+r^n/2} \frac{\xi}{[\xi^2 + (\eta - \tilde{\eta})^2 + (\zeta - \tilde{\zeta})^2]^{3/2}} d\tilde{\eta} d\tilde{\zeta}, \\ a^\xi &= \frac{\partial t / \partial \tau}{4\pi} \int_{-r^t/2}^{+r^t/2} \int_{-r^n/2}^{+r^n/2} \frac{2\xi^2 - (\eta - \tilde{\eta})^2 - (\zeta - \tilde{\zeta})^2}{[\xi^2 + (\eta - \tilde{\eta})^2 + (\zeta - \tilde{\zeta})^2]^{5/2}} d\tilde{\eta} d\tilde{\zeta}, \\ a^n &= \frac{\partial t / \partial \tau}{4\pi} \int_{-r^t/2}^{+r^t/2} \int_{-r^n/2}^{+r^n/2} \frac{3\xi(\eta - \tilde{\eta})}{[\xi^2 + (\eta - \tilde{\eta})^2 + (\zeta - \tilde{\zeta})^2]^{5/2}} d\tilde{\eta} d\tilde{\zeta}, \\ a^t &= \frac{\partial t / \partial \tau}{4\pi} \int_{-r^t/2}^{+r^t/2} \int_{-r^n/2}^{+r^n/2} \frac{3\xi(\zeta - \tilde{\zeta})}{[\xi^2 + (\eta - \tilde{\eta})^2 + (\zeta - \tilde{\zeta})^2]^{5/2}} d\tilde{\eta} d\tilde{\zeta}. \end{aligned} \quad (5.5)$$

After lengthy calculations the following, relatively simply, closed-form solutions for the pressure and acceleration fields due to the rectangular dipole element can be found:

$$\begin{aligned} P &= \rho \frac{\partial t / \partial \tau}{4\pi} [f^p(\xi, \eta^1, \zeta^1) - f^p(\xi, \eta^2, \zeta^2) - f^p(\xi, \eta^3, \zeta^3) + f^p(\xi, \eta^4, \zeta^4)] \\ a^\xi &= \frac{\partial t / \partial \tau}{4\pi} [f^\xi(\xi, \eta^1, \zeta^1) - f^\xi(\xi, \eta^2, \zeta^2) - f^\xi(\xi, \eta^3, \zeta^3) - f^\xi(\xi, \eta^4, \zeta^4)], \\ a^n &= \frac{\partial t / \partial \tau}{4\pi} [f^n(\xi, \eta^1, \zeta^1) - f^n(\xi, \eta^2, \zeta^2) - f^n(\xi, \eta^3, \zeta^3) - f^n(\xi, \eta^4, \zeta^4)], \\ a^t &= \frac{\partial t / \partial \tau}{4\pi} [f^t(\xi, \eta^1, \zeta^1) - f^t(\xi, \eta^2, \zeta^2) - f^t(\xi, \eta^3, \zeta^3) - f^t(\xi, \eta^4, \zeta^4)], \end{aligned} \quad (5.6)$$

where the arguments  $\xi, \eta^1, \zeta^1, \xi, \eta^2, \zeta^2$ , etc., relate to coordinate systems which are translated into the corner points 1, 2, ..., etc. of the dipole element.

$$\begin{aligned} \eta^1 &= \eta + r^n/2, & \eta^2 &= \eta - r^n/2, & \eta^3 &= \eta + r^n/2, & \eta^4 &= \eta - r^n/2, \\ \zeta^1 &= \zeta + r^l/2, & \zeta^2 &= \zeta + r^l/2, & \zeta^3 &= \zeta - r^l/2, & \zeta^4 &= \zeta - r^l/2. \end{aligned}$$

The functions  $f^y, f^\xi, f^\eta, f^l$  are defined as follows:

$$\begin{aligned} f^y(x, y, z) &= \arctan \frac{yz}{x(x^2 + y^2 + z^2)^{1/2}} \quad (\text{principal value}); \\ f^\xi(x, y, z) &= \frac{yz(2x^2 + y^2 + z^2)}{(x^2 + y^2)(x^2 + z^2)(x^2 + y^2 + z^2)^{1/2}}, \\ f^\eta(x, y, z) &= \frac{-xz}{(x^2 + y^2)(x^2 + y^2 + z^2)^{1/2}}, \\ f^l(x, y, z) &= \frac{-xy}{(x^2 + z^2)(y^2 + y^2 + z^2)^{1/2}}. \end{aligned} \tag{5.7}$$

## 6. DISCUSSION OF THE FIELDS DUE TO A RECTANGULAR DIPOLE ELEMENT

In order to study the properties of the pressure field described by Eqs. (5.6) the close environment of the plane  $\xi = 0$  will be investigated. Defining the location of a field point by the angle  $\alpha$ , as shown in Fig. 4, the formula for the pressure can be approximated by

$$P = \left( \frac{1}{2} - \frac{\alpha}{2\pi} \right) \rho \frac{\partial t}{\partial \tau} \quad \text{for } |\xi| \ll r^l. \tag{6.1}$$

Based on this relation the following statements can easily be verified:

—Approaching the dipole element from the half space  $\xi > 0$  the limit pressure is

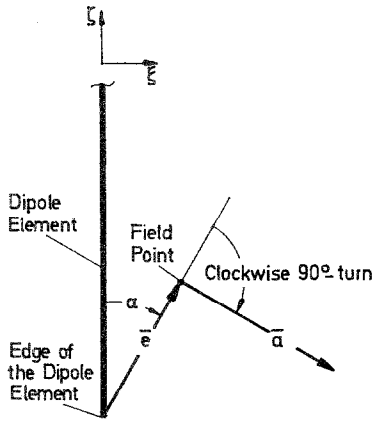
$$\lim_{\xi \rightarrow +0} P = \frac{1}{2} \rho \frac{\partial t}{\partial \tau}.$$

Approaching the dipole element from the half space  $\xi < 0$  the limit has the opposite sign. However, for the plane  $\xi = 0$  outside the dipole element, the pressure  $P$  vanishes (Fig. 5).

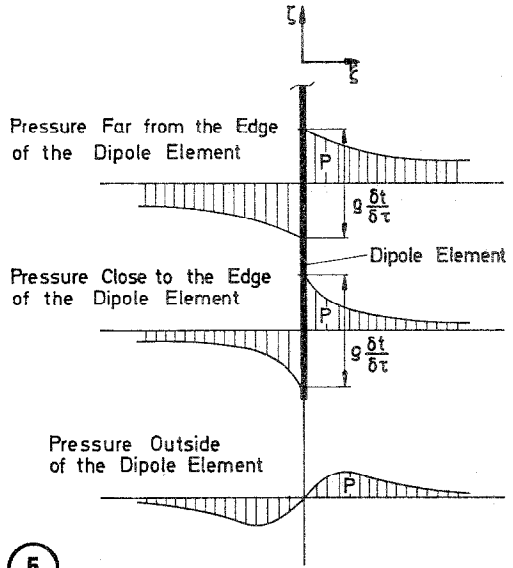
Thus, within the dipole element a pressure step

$$\Delta P = \rho \frac{\partial t}{\partial \tau}$$

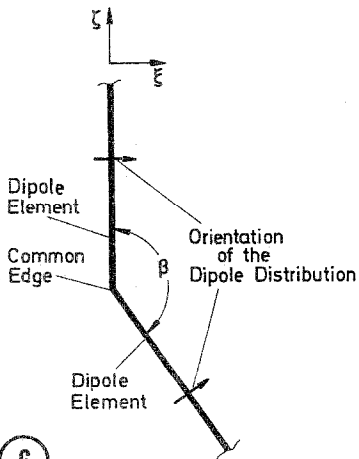
occurs which may be used to simulate pressure differences across thin walls wetted on both sides.



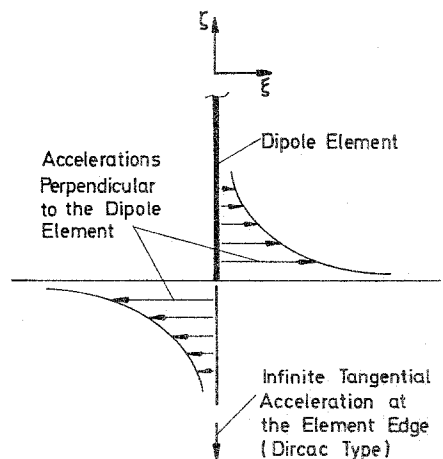
4



5



6



7

FIG. 4. Coordinates of a field point close to the edge of a dipole element.

FIG. 5. Pressure distributions perpendicular to the plane of the dipole element.

FIG. 6. Two joining dipole elements with the angle  $\beta$ .

FIG. 7. Accelerations at the dipole element.

—For two dipole elements having a common edge and the same dipole intensities but different orientations (Fig. 6), approaching the edge from opposite dipole directions yields the limit pressures

$$\lim_{+\beta} P = \left(1 + \frac{\beta}{2\pi}\right) \rho \frac{\partial t}{\partial \tau},$$

and approaching the edge from the other side, yields the limit pressure of

$$\lim_{-\beta} P = \left(1 - \frac{\beta}{2\pi}\right) \rho \frac{\partial t}{\partial \tau},$$

so that also close to edges between two dipole elements, the pressure step within the elements is

$$\Delta P = \rho \frac{\partial t}{\partial \tau}.$$

This is true even for elements with different dipole intensities.

Also the equations for the acceleration vector close to the edge of the dipole element become very simple. Defining the location of a field point by the distance  $|\bar{e}|$  and the angle  $\alpha$ , as shown in Fig. 4, the acceleration vector has a value of

$$|\bar{a}| = \frac{1}{\pi} \frac{\partial t}{\partial \tau} \frac{1}{|\bar{e}|}. \quad (6.2)$$

The direction is obtained by a clockwise  $90^\circ$  turn of the distance vector  $\bar{e}$ .

From these findings it follows immediately:

—Inside the dipole element the acceleration vector is perpendicular to the element plane. Approaching the edges of the dipole element the acceleration vector approaches an infinite value hyperbolically. However, at the edges the acceleration component perpendicular to the element plane vanishes and an infinite component tangential to the element plane (and perpendicular to the element edge) occurs (Fig. 7).

It follows that in the edge region of the dipole element the acceleration perpendicular to the element plane has a vanishing mean value. Consequently, in cases where, according to the boundary conditions, no flow (or prescribed flow) perpendicular to the dipole element should occur, this requirement is violated only locally, in regions one order of magnitude smaller than the dipole elements. But on average the requirement will be satisfied, provided it is satisfied at the center point of the dipole element.

However, the mean value of the tangential acceleration in the edge region of the dipole element does not vanish. Rather the infinite tangential acceleration at the edge is of Dirac type and the integral over this singularity is

$$\int a^{\zeta} d\zeta = \frac{\partial t}{\partial \tau}.$$

(In order to carry through this integration an integration path in  $\zeta$  direction but at a small distance from the dipole element may be used.)

Therefore the infinite tangential acceleration at the element edge has an effect which is not only local, so that the tangential acceleration at the center of the dipole element is not an appropriate representation of the flow in  $\zeta$ -direction.

—For two dipole elements having a common edge and the same dipole intensities but different orientations the infinite accelerations at the common edge cancel each other. For elements with different dipole intensities the remaining infinite acceleration generates a vortex flow with the common edge as axis.

Consequently, if a curved surface is formed by dipole elements, uncontrolled leakages due to the element edges have only a local character, related to regions one order of magnitude smaller than the dipole elements. On average the leakage at the element edges vanishes. This is an important advantage in comparison to elements with distributed sources where large leakages have been observed, for instance by Renken [21].

#### 7. SUPERPOSITION OF THE FIELDS DUE TO RECTANGULAR DIPOLE ELEMENTS AND DISCRETE SOURCES

As stated by Lamb [28] and mentioned in [7], for instance, any irrotational, inviscid, and incompressible flow without sources and volume forces may be generated by appropriate source and dipole distributions over the fluid field boundary. In almost all applications so far, only source distributions have been used, for simplicity. In this paper, however, the singularity distribution over the fluid boundary is modeled primarily by dipole elements and use is made of the advantages of these elements, discussed in the preceding section. Sources concentrated in discrete points may be used exceptionally in special problems. Consequently in this work the method described in [20] is included as an option. The way in which the dipole elements and point sources are specified and the superposition of the corresponding pressure and acceleration fields is described in this section. Further details may be found in [29].

The geometry of the fluid boundary as well as the size, location, and orientation of the rectangular dipole elements, and, if applicable, the location of the discrete sources will be related to a global Cartesian coordinate system  $x, y, z$ . Within this system, points

numbered by	$i = 1, 2, \dots, I$
and described by their position vector	$r_j = (x_j, y_j, z_j)$ ,
attached tangential vectors	$\bar{r}_j^n = (x_j^n, y_j^n, z_j^n)$ , $\bar{r}_j^k = (x_j^k, y_j^k, z_j^k)$ ,
the boundary values	$a_j^b$ or $P_j^b$ ,
and some additional quantities	$i_j^1, i_j^2$ , $k_j^1, k_j^2, k_j^3, k_j^4$ , $g_j^1, g_j^2, g_j^3, g_j^4$

may be given. Depending on the indicators  $i_j^1$  and  $i_j^2$  the point  $j$  and the related quantities describe a boundary point and the type of the boundary conditions, or a singularity, or both. In this way the data input for specification and solution of a problem has been minimized.

The indicator  $i_j^1$  means:

- $i_j^1 = 1$  The point  $j$  is a boundary point and the vectors  $\bar{r}_j^n$  and  $\bar{r}_j^\xi$  are tangential vectors of the boundary surface, or the point  $j$  is a field point.
- $i_j^1 = 2$  The point  $j$  is the center of a rectangular dipole element and the vectors  $\bar{r}_j^n$  and  $\bar{r}_j^\xi$  denote length and width of the element as well as the basic vectors of the local Cartesian coordinate system  $\xi, \eta, \zeta$  related to this element.
- $i_j^1 = 3$  The point  $j$  denotes a concentrated source (which is used as a singularity for solving the problem).
- $i_j^1 = 0$  The point  $j$  is both a boundary point and the center of a dipole element (combination of  $i_j^1 = 1$  and  $i_j^1 = 2$ ).

The case  $i_j^1 = 1$  together with  $i_j^1 = 2$  allows application of the technique of "submerged" dipole elements as indicated in Fig. 8. The case  $i_j^1 = 1$  together with  $i_j^1 = 3$  allows for applying of point sources as singularities in order to solve the problem. In both cases the singularities (dipole elements, point sources) have a certain distance from the fluid field. In the standard case of  $i_j^1 = 0$  the boundary surface is formed by rectangular dipole elements and care must be taken that leakages and overlappings between adjacent elements are minimized, as shown in Fig. 9 for instance.

The indicator  $i_j^2$  means:

- $i_j^2 = 0$  At point  $j$  the pressure and acceleration will be calculated.
- $i_j^2 = 2$  The point  $j$  is a boundary point with given normal acceleration  $a_j^b$  (acceleration perpendicular to the boundary surface). The pressure at point  $j$  will be calculated.
- $i_j^2 = 3$  The point  $j$  is a boundary point with given pressure  $P_j^b$ . The acceleration at this point will be calculated.

The indicators  $k_j^1, \dots, k_j^4$  and the related weights  $g_j^1, \dots, g_j^4$  allow reduction of the number of unknowns describing the singularity distribution in comparison to the number of dipole elements or source points. Denoting these unknowns by

$$X_k, \quad k = 1, 2, \dots, K, \quad K = \text{Max}(k_j^1, k_j^2, k_j^3, k_j^4), \quad j = 1, 2, \dots, J,$$

the uniform intensity of the dipole element  $j$  or the strength of the source point  $j$  is

$$\frac{\partial t_j / \partial \tau}{\partial S_j / \partial \tau} \Big\} = 4\pi(g_j^1 X_{k_j^1} + g_j^2 X_{k_j^2} + g_j^3 X_{k_j^3} + g_j^4 X_{k_j^4}). \quad (7.1)$$

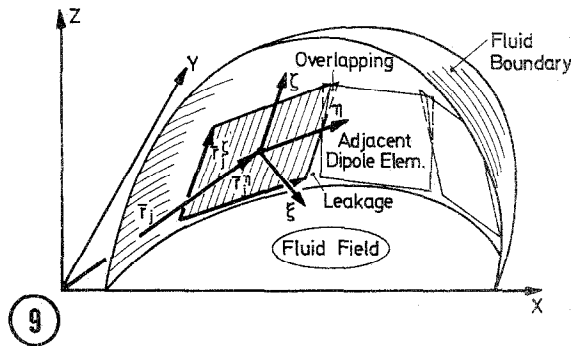
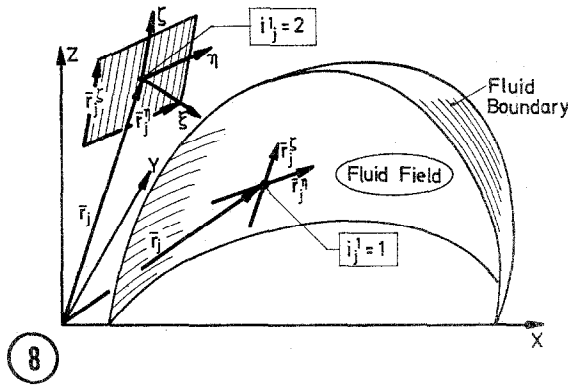
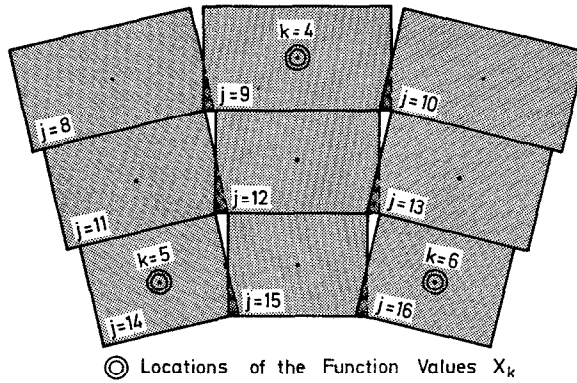


FIG. 8. Boundary point ( $i_j^1 = 1$ ) and "submerged" dipole element ( $i_j^1 = 2$ ).

FIG. 9. Dipole elements forming the fluid boundary ( $i_j^1 = 0$ ).

The indicators  $k_j^1, \dots, k_j^4$  and the related weights  $g_j^1, \dots, g_j^4$  may be specified from the following considerations:

Assign the unknowns  $X_k$  to locations spread all over the fluid boundary and interpret the unknowns as function values describing the intensities of the singularities in the environment of these locations. To each function value a boundary point should be assigned where either the acceleration  $a_j^b$  or the pressure  $P^b$  is prescribed, i.e.,  $i_j^2 = 2$  or 3. In regions where relatively sharp gradients are expected or high accuracy is required more function values, more prescribed pressures or accelerations, and more dipole elements or source points should be used than in other regions. For each dipole element or point source  $j$  find one, two, three, or four adjacent function values  $X_k$  with the indices  $k = k_j^1, \dots, k_j^4$ . Then choose appropriate weights  $g_j^1, \dots, g_j^4$  in order to determine the intensity of the dipole element  $j$  or the strength of the source point  $j$  by interpolation with Eq. (7.1). Usually the weights should be approximately inversely proportional to the distance between the dipole element or source point



Chosen Values:

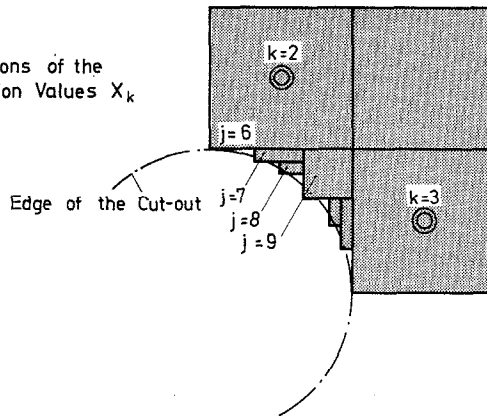
Dipole Element 9  
 $k_9^1 = 4$   
 $g_9^1 = 1.$

Dipole Element 12  
 $k_{12}^1 = 4$     $k_{12}^2 = 5$     $k_{12}^3 = 6$   
 $g_{12}^1 = 0.5$     $g_{12}^2 = 0.25$     $g_{12}^3 = 0.25$

Dipole Element 15  
 $k_{15}^1 = 5$     $k_{15}^2 = 6$   
 $g_{15}^1 = 0.5$     $g_{15}^2 = 0.5$

10

$\odot$  Locations of the Function Values  $X_k$



Chosen Values:

Dipole Element 6

Dipole Element 7

Dipole Element 8

Dipole Element 9

$y_6 = \dots$     $y_7 = \dots$     $y_7 = \dots$     $y_8 = \dots$     $y_8 = \dots$     $y_9 = \dots$     $y_9 = \dots$

11

FIG. 10. The indicators  $k_j^1, \dots$  and related weights  $g_j^1, \dots$  for a smoothly curved fluid boundary.

FIG. 11. The indicators  $k_j^1, \dots$  and related weights  $g_j^1, \dots$  for a fluid boundary with a cutout.



and the position of the corresponding function values. But never use the same function value to determine both the intensity of a dipole element and the strength of a point source. Two examples of the choice of appropriate indicators  $k_j^1, \dots$  and related weights  $g_j^1, \dots$  are presented in Fig. 10 and 11. The standard case with one unknown for each singularity, which is assumed in all other known methods, is obtained with  $k_j^1 = j$  and  $g_j^1 = 1$ .

For a unique solution of the problem, the number  $K$  of the unknowns must be smaller than or equal to the number of singularities ( $i_j^1 = 0$  or 2 or 3), and equal to the number of boundary points with prescribed acceleration  $a_j^b$  or pressure  $P_j^b$  ( $i_j^1 = 0$  or 1,  $i_j^2 = 2$  or 3).

As an additional option inside the fluid field discrete sources with prescribed intensities can be taken into account. Strictly, these source points no longer belong to the fluid region. Instead small spheres surrounding these sources may be interpreted as additional fluid boundaries with the source intensities as boundary conditions.

The superposition of the pressure and acceleration fields due to the singularities is straightforward. For any point  $l$  where pressure and acceleration are to be calculated the local coordinates  $\xi, \eta, \zeta$  with respect to each dipole element and the distance to each source point have to be determined. Then the formulas (5.6) with (5.7) or (5.3), respectively, can be applied. Before summation of the accelerations, due to the different singularities, retransformation to the global coordinate system  $x, y, z$  is necessary, where the components of the acceleration vector  $\bar{a}$  are  $a^x, a^y, a^z$ . Now the superimposed pressure  $P$  and acceleration  $\bar{a}$  at point  $l$  are

$$\begin{aligned} P &= B_l^P + \sum_{k=1}^K C_{lk}^P X_k, & a^y &= B_l^y + \sum_{k=1}^K C_{lk}^y X_k, \\ a^x &= B_l^x + \sum_{k=1}^K C_{lk}^x X_k, & a^z &= B_l^z + \sum_{k=1}^K C_{lk}^z X_k. \end{aligned} \quad (7.2)$$

The coefficients  $C_{lk}^P, C_{lk}^x, \dots$  are determined by the above procedure and describe the influence of the function values of the singularities on pressure and acceleration at point  $l$ . The terms  $B_l^P, B_l^x, \dots$  arise from the discrete sources with prescribed intensities inside the fluid field.

## 8. SATISFACTION OF THE BOUNDARY CONDITIONS BY DETERMINATION OF INTENSITIES OF THE SUPERIMPOSED SINGULARITIES

Satisfaction of the boundary conditions means that at each specified boundary point with  $i_j^1 = 0$  or 1 and  $i_j^2 = 2$  or 3, either the normal component of the acceleration  $\bar{a}$  assumes the given value  $a_j^b$  or the pressure  $P$  assumes the given value  $P_j^b$ . Consequently, from (7.2) the following system of linear equations for the unknowns  $X_k$  is obtained:

For  $i_j^1 = 0$  or 1 and  $i_j^2 = 2$  (prescribed normal acceleration)

$$\sum_{k=1}^K C_{jk}^\epsilon X_k = a_j^b - B_j^\epsilon.$$

For  $i_j^1 = 0$  or 1 and  $i_j^2 = 3$  (prescribed pressure) (8.1)

$$\sum_{k=1}^K C_{jk}^P X_k = P_j^b - B_j^P.$$

In the former system the coefficient  $C_{jk}^\epsilon$  and the term  $B_j^\epsilon$  result from  $C_{jk}^x$ ,  $C_{jk}^y$ ,  $C_{jk}^z$  and  $B_j^x$ ,  $B_j^y$ ,  $B_j^z$ , respectively, when, based on Eqs. (7.2), the normal acceleration  $a_j^\epsilon$  is calculated from the components  $a^x$ ,  $a^y$ ,  $a^z$ . The normal directions of the specified boundary points are given by the cross product  $\bar{r}_j^n \times \bar{r}_j^\epsilon$ .

Since the number  $K$  of the unknowns  $X_k$  was chosen to be equal to the number of boundary points with prescribed pressure or normal acceleration, the equation systems (8.1) include as many linear equations as unknowns. Provided the physical problem to be investigated is reasonable, which means, for instance, that the fluid boundary includes at least one region with prescribed pressure, the linear equations are independent of each other. Under these conditions a unique solution for the unknowns  $X_k$  may be obtained by standard procedures.

For physical problems where the boundary regions with prescribed pressures are relatively small (for example a rigid-wall fluid container with relatively small openings) numerical problems may occur due to ill-conditioned coefficient matrices. However, by applying dipole elements with a faster decay behavior than source elements it may be concluded that this class of awkward problems is not very significant. (For problems with flexible boundaries this restriction does not exist.)

Once the singularity distribution described by the function values  $X_k$  is known, the flow conditions at any given fluid point, i.e., the pressure and accelerations, can be calculated immediately by Eqs. (7.2). This is particularly easy for the specified boundary points because the coefficients  $C_{lk}^P, \dots$  and the terms  $B_l^P, \dots$  are known anyway from preceding calculations. For other fluid points the determination of the corresponding coefficients and terms represents an additional effort.

## 9. IMPLEMENTATION OF THE COMPUTER PROGRAM SING1

The computer program SING1 is based on the theory described above. It is assumed that the problems may be symmetric about the plane  $z = 0$ , and information need be given for only one of the symmetric parts. The generality is not reduced by this assumption since nonsymmetric problems can be defined completely within the region  $z > 0$ . The symmetry condition then means that the problem is solved twice, in the region  $z > 0$  and in the region  $z < 0$ .

The size of the problems, i.e., the number of boundary points and singularities, is not limited by the program but only by the available memory space and the CPU time of the computer. The program is written in PL/1 and the input may be given in free format. The input data are essentially the same as those listed in the section before. The symbols used in the program are also identical or very close to the symbols used in this paper.

SING1 consists of the following modules:

SIDIAG	Reading, checking and rearranging of the input data.
SIPLOT	Control plot of the geometrical structure including the specified boundary points and the singularities.
SIKOEf	Calculation of the coefficients $C_{ik}^P, \dots$ and the terms $B_i^P, \dots$ and preparation of the linear equation system for the unknowns $X_k$ .
SISOLV	Solution of the linear equation system and calculation of pressure and accelerations at specific points (boundary points and, if required, field points).
SIPLOT	Plot of the results.

As an indication of the computational effort of SING1 the memory space and the CPU time used for examples 1 and 2 discussed in the next section are given:

	Example 1 (T-joint)	Example 2 (water pool of a pressure suppression system)
CPU time	35 sec	17 min
Memory space	190 kbyte	1000 kbyte

## 10. APPLICATIONS

In order to demonstrate the applicability of the method, two different examples have been solved with SING1. In both cases the singularity distribution was provided by dipole elements located at the fluid boundary.

The first example is the incipient flow in a T-joint with rectangular surfaces and cross sections. The modeling of this fluid boundary by rectangular dipole elements is very simple and is shown in Fig. 12. The problem is symmetric about the plane  $z = 0$  which is automatically taken into account by the code SING1. Furthermore the

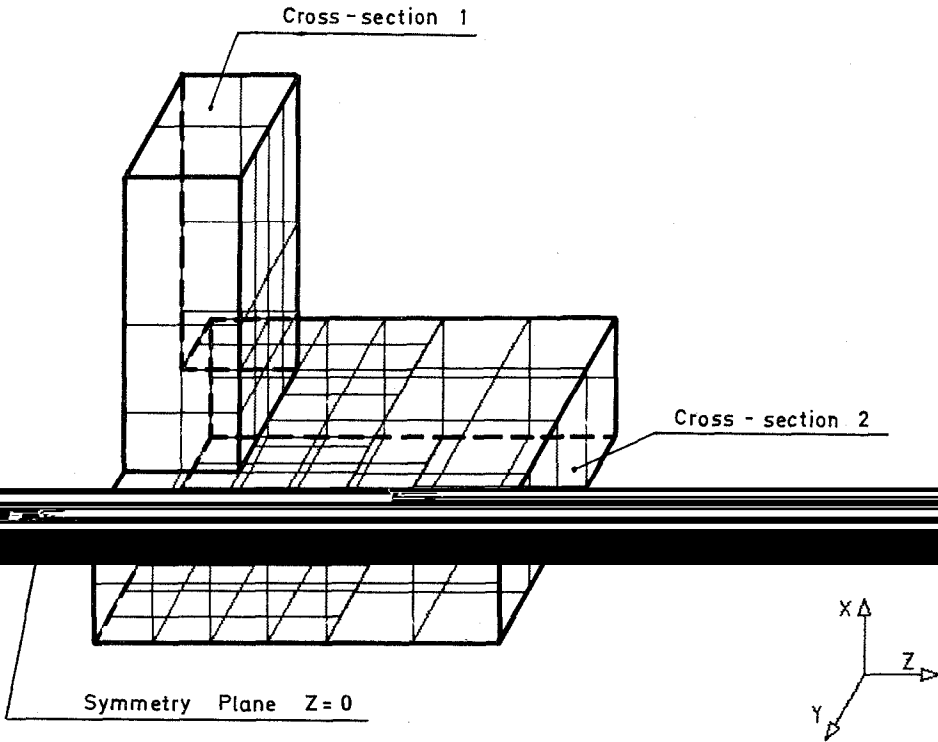


FIG. 12. Boundary discretization of a T-joint with different rectangular cross sections.

problem is symmetric about the plane  $y = 0$ , so independent function values  $X_k$  for the singularity distribution are specified only at the centers of those dipole elements which are located in the region  $y > 0$ . In this way only 63 unknowns were necessary although the number of dipole elements used was 126. A further reduction of the number of unknowns by using the same function value  $X_k$  for several adjacent dipole elements was not made in this example. Cross section 1 with a prescribed pressure of 3 bars and cross section 2 with vanishing pressure form the openings of the T-joint. The remaining fluid boundaries are rigid walls. The pressure distribution over these walls and the normal accelerations at cross sections 1 and 2 have been calculated with SING1. The result immediately after flow begins is shown in Fig. 13, where the lengths of the horizontal lines are proportional to the pressure and the lengths of the vertical lines with arrows are proportional to the normal acceleration at the particular surfaces. Despite the sharp edges and the relatively small number of dipole elements and unknowns the results seem to be satisfactory. The ratio of the accelerations in cross sections 1 and 2 calculated with SING1 differs by less than 0.5% from the exact value. Therefore it may be concluded that essential fluid losses due to leakages at edges, which had been observed in calculations with other singularity methods [21], do not occur in SING1.

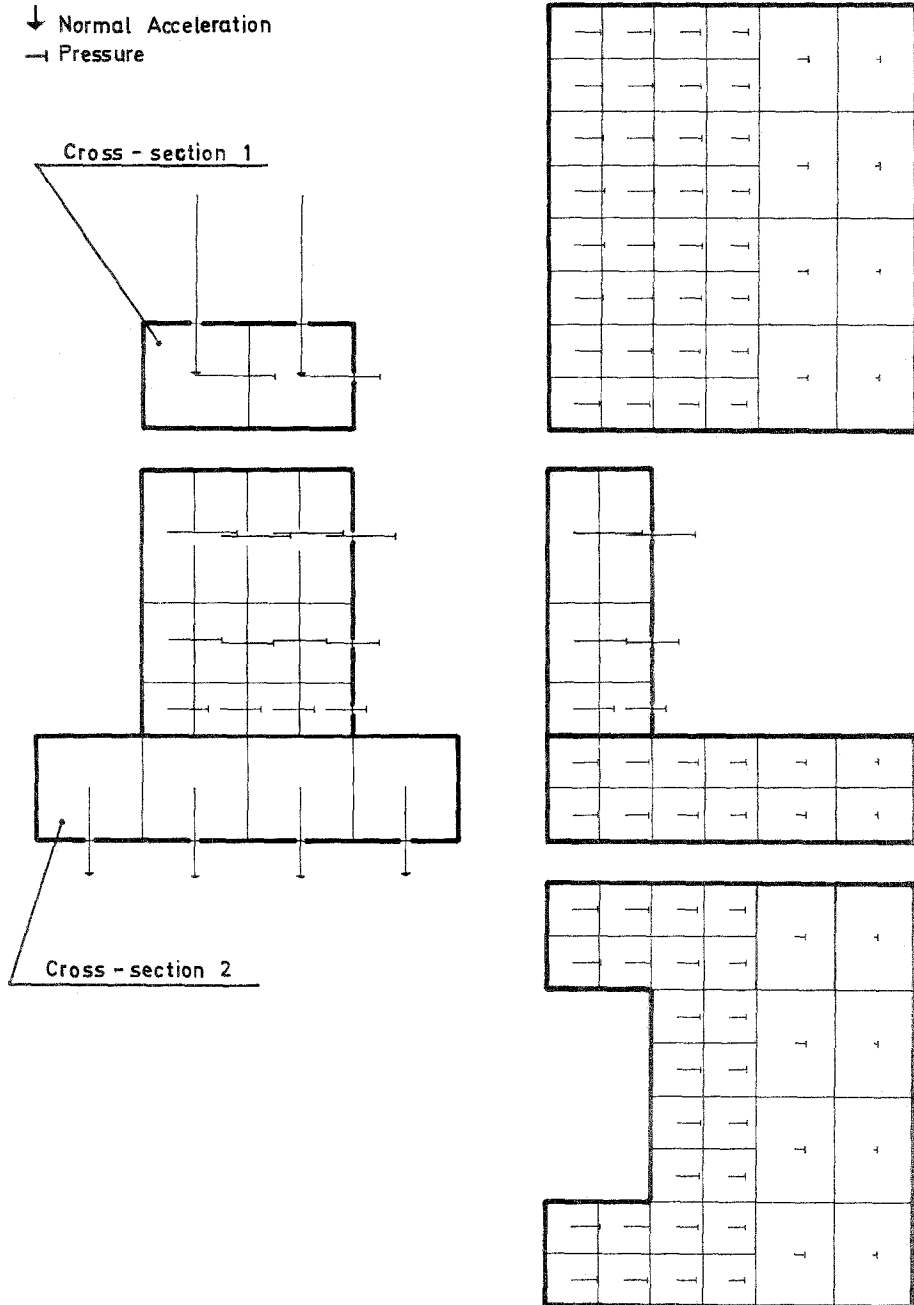


FIG. 13. Pressure and acceleration distribution over the surfaces and cross sections of a T-joint.

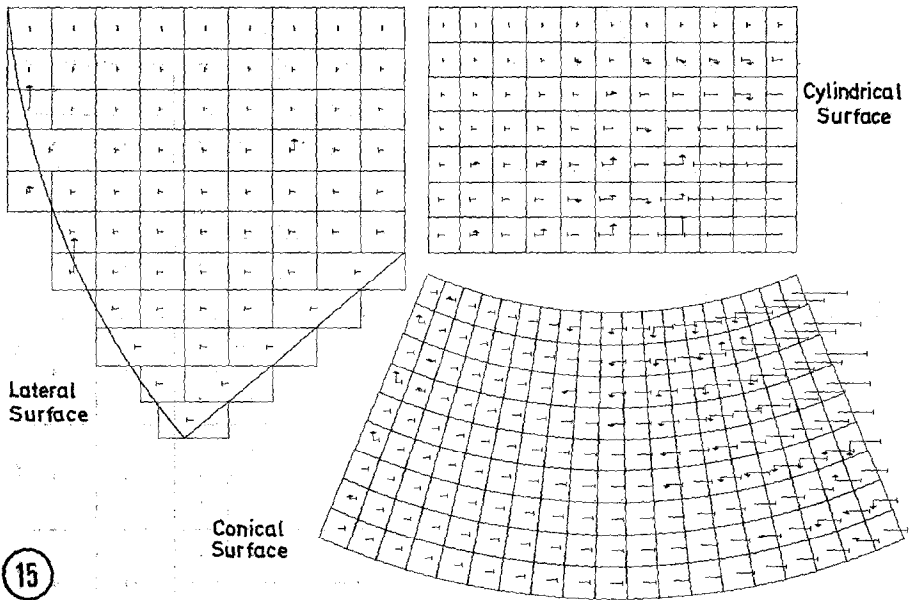
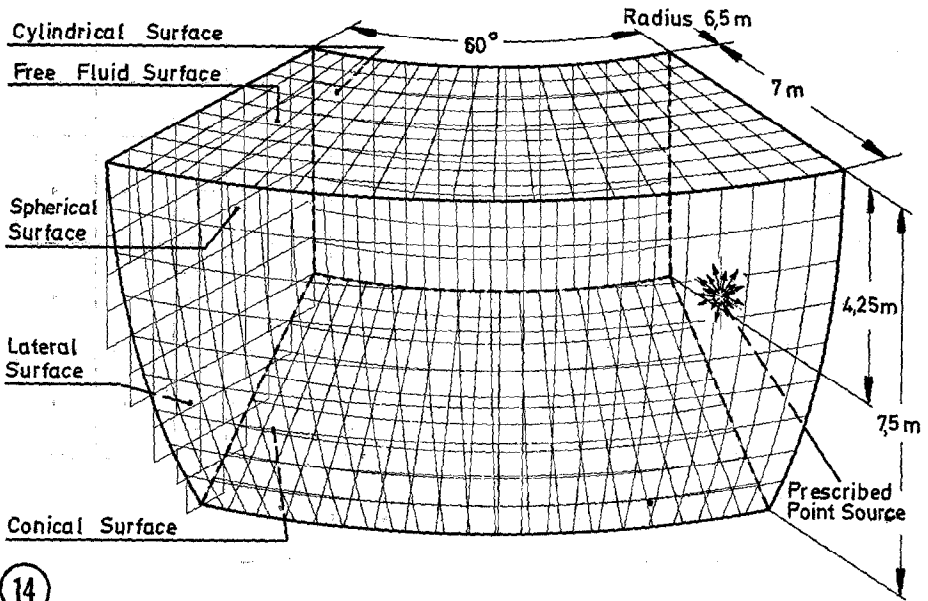


FIG. 14. Boundary discretization of a 60° section of the pressure suppression system.

FIG. 15. Pressure distribution over the cylindrical, lateral, and conical surface.

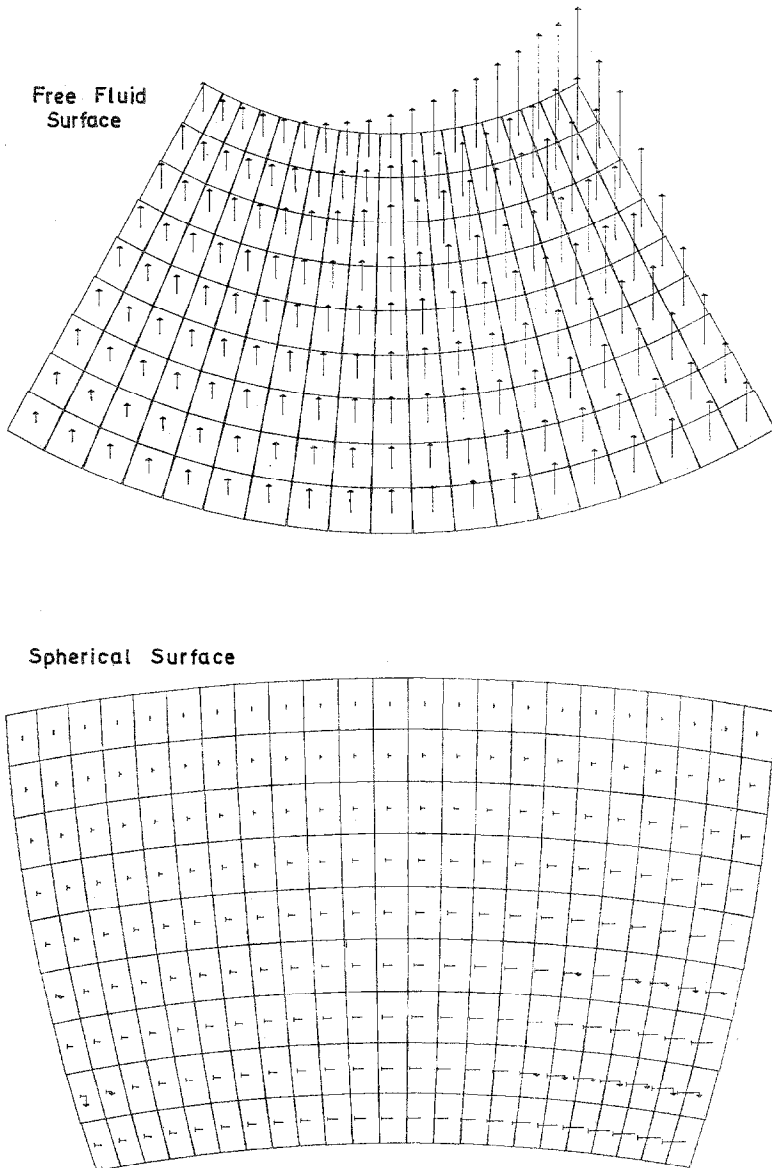


FIG. 16. Pressure and acceleration distribution over the free fluid surface and spherical surface.

The second example is the oscillating flow in the water pool of the pressure suppression system of a boiling water reactor. Under certain operating or emergency conditions steam is blown into the water pool through downcomer tubes. At the end of these tubes highly transient condensation processes may take place causing pulsating

flows and pressures in the whole system. The fluctuating pressure distributions at the walls are significant for the structural integrity of the system. Figure 14 shows a 60° section of the water pool. The transient condensation process is represented by a fluid source with a given intensity gradient. At all surfaces the normal acceleration vanishes except at the free water surface. Here the pressure vanishes. This means that the walls of the water pool are assumed to be rigid. The discretization of the fluid boundary by a total of 696 dipole elements is also shown in Fig. 14. It can be seen that the overlappings and leakages between the dipole elements are rather small. Using the same function value  $X_k$  for several adjacent dipole elements the number of unknowns was reduced to a total of 247. The results obtained with SING1 are shown in Figs. 15 and 16. As in the first example the lengths of the horizontal lines are proportional to the pressures and the lengths of the vertical lines with arrows are proportional to the accelerations at the centers of the dipole elements. Acceleration lines smaller than the length of the arrow are omitted. Since satisfaction of the boundary conditions was not required at the center of each dipole element small accelerations perpendicular to the walls occur, representing the actual boundary conditions.

In more detailed investigations calculations have been carried through with a slightly different set of function values and different locations of the prescribed fluid sources. The results are reported in [29]. They indicate that local errors in the boundary conditions have very little influence on the pressure distribution.

The same examples 1 and 2 but with one wall flexible will be investigated in the second part of this paper.

#### REFERENCES

1. D. J. F. EWING, Analysis of pressure-transients using incompressible flow theory, Second Int. Conf. on Pressure Surges, London, Sept. 22-24, 1976.
2. L. M. DELVES AND J. WALSH, "Numerical Solution of Integral Equations," Oxford Univ. Press. (Clarendon), London, 1974.
3. J. L. HESS AND A. M. O. SMITH, *Progr. Aeronaut. Sci.* **8** (1967), 1-138.
4. J. L. HESS, *Comput. Meth. Appl. Mech. Eng.* **5** (1975), 145-196.
5. J. L. HESS, *Comput. Meth. Appl. Mech. Eng.* **5** (1975), 297-308.
6. B. L. HEWITT *et al.*, Computational methods and problems in aeronautical fluid dynamics, in "Proceedings, Conf. Univ. of Manchester, London, 1976."
7. F. T. JOHNSON AND P. E. RUBBERT, Advanced panel-type influence coefficient method applied to subsonic flows, AIAA 13th Aerospace Science Meeting, Pasadena, Calif., Jan. 20-27, 1975, paper 75-50.
8. R. T. MEDAN, Overview of the NASA-Ames three-dimensional potential flow analysis system (POTFAN), to be published.
9. E. GRODTKJAER, *Int. J. Num. Meth. Eng.* **6** (1973), 253-264.
10. H. KÖRNER AND E. H. HIRSCHL, *J. Fluid Mech.* **79** (1975), 181-189.
11. A. EGER, J. EICHERS, AND T. BRATANOW, *J. Hydronaut.* **9** (1975), 64-68.
12. W. ALBRING AND G. SCHINDLER, *Maschinenbautechnik* **23** (1974).
13. W. C. WEBSTER, *J. Ship Res.* **19** (1975), 206-219.
14. J. H. ARGYRIS AND D. W. SCHARPF, *Aeronaut. J. Roy. Aeronaut. Soc.* **73** (1969), 959-961.



15. J. C. NEDLEC, Curved finite element methods for the solution of integral singular equations on surfaces in  $R^3$ , in "Computing Methods in Applied Sciences and Engineering," Proceedings, Second Int. Symp., Dec. 15-19, 1975, Springer-Verlag, New York/Berlin, 1976.
16. B. MASKEW, "A Submerged Singularity Method for Calculating Potential Flow Velocities at Arbitrary Near-Field Points," NASA TMX-73115, 1976.
17. G. DE MEY, *Computers and Structures* **8** (1978), 113-115.
18. H. K. HÖLLER, *Escher Wyss Mitt.* **45** (1972), 1.
19. L. LANDWEBER, *Hydronautics* **8** (1974), 137-145.
20. R. KRIEG, Nonsymmetric transient pressure load on reactor vessel caused by point sources simulating fuel sodium interaction, ANS Conf. Fast Reactor Safety, Beverly Hills, Calif., April 2-4, 1974.
21. J. RENKEN, Untersuchung der dreidimensionalen Strömung in einem Kanal mit rechteckigem, variablem Querschnitt mit Hilfe des Panel-Verfahrens, Deutsche Forschungs- und Versuchsanstalt für Luft- und Raumfahrt, Köln, Forschungsbericht 75-46, 1975.
22. A. A. AMSDEN, C. W. HIRT, AND J. L. COOK, *J. Computational Physics* **14** (1974), 227.
23. U. SCHUMANN AND R. A. SWEET, Direct Poisson equation solver for potential, and pressure fields on a staggered grid with obstacles, Lecture Notes in Physics, Vol. 59, pp. 398-403, Springer/New York (1976).
24. U. SCHUMANN, "Instationäre Potentialströmung inkomplexer Geometrie am Beispiel von DWR-Blowdown Strömungen," Kernformungszentrum Karlsruhe, KfK 2324, 1976.
25. R. MEYDER, *J. Computational Physics* **17** (1975), 53-67.
26. F. C. THAMES, J. F. THOMPSON, C. W. MASTIN, AND R. L. WALKER, *J. Computational Physics* **24** (1977), 245-273.
27. R. KRIEG, "Three Dimensional Flow Fields Caused by Transient Dipoles Uniformly Distributed on Rectangular Plane Elements," Kernforschungszentrum Karlsruhe, KfK-Ext. 8/76-2, 1976.
28. H. LAMB, "Hydrodynamics," Cambridge Univ. Press, Cambridge, 1963.
29. R. KRIEG AND G. HAILFINGER, "SING1-ein Computercode zur Berechnung transienter, dreidimensionaler, inkompressibler Potentialströmungen nach dem Singularitätenverfahren," Kernforschungszentrum Karlsruhe, KfK 2505, 1978.